Simulation of $\tilde{A}\,^1B_1 \rightarrow \tilde{X}\,^1A_1$ CF_2 single vibronic level emissions: Including anharmonic and Duschinsky effects

Foo-Tim Chau[a)]
Department of Applied Biology and Chemical Technology, Hong Kong Polytechnic University, Hung Hom, Kowloon, Hong Kong

John M. Dyke and Edmond P. F. Lee
Department of Chemistry, University of Southampton, Highfield, Southampton SO17 1BJ, United Kingdom

Daniel K. W. Mok
Department of Applied Biology and Chemical Technology, Hong Kong Polytechnic University, Hung Hom, Kowloon, Hong Kong

(Received 18 June 2001; accepted 10 July 2001)

CASSCF/MRCI/aug-cc-pVQZ(no *g*) and RCCSD(T)/aug-cc-pVQZ potential energy functions were reported for the $\tilde{A}\,^1B_1$ and $\tilde{X}\,^1A_1$ states of CF_2, respectively. Vibrational wave functions of the symmetric stretching and bending modes of the two states of CF_2 were obtained in variational calculations, employing Watson's Hamiltonian for a nonlinear molecule and anharmonic vibrational wave functions expressed as linear combinations of harmonic basis functions. Franck–Condon factors (FCFs) were computed for $\tilde{A}\,^1B_1 \rightarrow \tilde{X}\,^1A_1$ CF_2 single vibronic level (SVL) emissions and the SVL emission spectra were simulated with the computed FCFs. When compared with the observed spectra, the simulated spectra obtained in the present investigation, which include allowance for anharmonicity and the Duschinsky effect, were found to be significantly superior to those reported previously, based on the harmonic oscillator model. Using the iterative Franck–Condon analysis procedure, with the geometry of the $\tilde{X}\,^1A_1$ state fixed at the recently determined experimental equilibrium geometry, the geometry of the $\tilde{A}\,^1B_1$ state of CF_2, which gave the best match between simulated and observed spectra, was found to be $r_e(\mathrm{CF}) = 1.317$ Å and $\theta_e(\mathrm{FCF}) = 121.25°$.
 [DOI: 10.1063/1.1398103]

I. INTRODUCTION

Recently, we have reported simulated spectra of $\tilde{A}\,^1B_1 \rightarrow \tilde{X}\,^1A_1$ CF_2 single vibronic level (SVL) emissions, employing our Franck–Condon factor (FCF) code, CART-FCF. This is based on the harmonic oscillator model and includes Duschinsky rotation (see Ref. 1 for details). The observed $\tilde{A}\,^1B_1 \rightarrow \tilde{X}\,^1A_1$ CF_2 SVL emissions consist of very long vibrational progressions in the bending mode. Comparison between the simulated[1] and observed spectra[2] led to the conclusion that the harmonic oscillator model employed in the simulations was inadequate for high vibrational levels of the $\tilde{X}\,^1A_1$ state involved in the electronic transition. Recently, we have reviewed existing FCF methods, which include anharmonic effects.[1,3] In a prior article,[1] a simple approach of incorporating anharmonicity in multidimensional FCF calculations was proposed. In a later article,[3] we reported our recently developed AN-FCF code, which includes both anharmonicity and Duschinsky effects, and its first application to the simulation of the He I photoelectron spectrum of ClO_2. In the present study, with the AN-FCF code, we present significantly improved simulated spectra of $\tilde{A}\,^1B_1 \rightarrow \tilde{X}\,^1A_1$ CF_2 SVL emissions, employing CASSCF/MRCI/aug-cc-pVQZ(no *g*) and RCCSD(T)/aug-cc-pVQZ potential energy functions (PEFs) of the two electronic states involved.

Earlier experimental and theoretical studies on the $\tilde{A}\,^1B_1$ and $\tilde{X}\,^1A_1$ states of CF_2, which have been discussed in Ref. 1, will not be repeated here. Nevertheless, a few very recent publications, which are relevant to the present study, should be mentioned. Firstly, Margules *et al.*[4] derived equilibrium geometrical parameters of the $\tilde{X}\,^1A_1$ state of CF_2 from experimental rotational constants (A_e and B_e), which were reported in previous high-resolution spectroscopic studies,[5–7] giving values of 1.2975 Å and 104.81° for r_e(CF) and θ_e(FCF), respectively. These authors also estimated the equilibrium geometrical parameters of r_e and θ_e as 1.297(2) Å and 104.78(2)°, respectively, from the highly reliable averaged geometrical parameters of $r_{av} = 1.3035 \pm 0.0001$ Å and $\theta_{av} = 104.778 + 0.02/-0.008°$ (Ref. 8). These two sets of experimentally derived equilibrium geometrical parameters agree well with each other and also with the best *ab initio* estimates of 1.2972 Å and 104.858° available at that time [at the RCCSD(T)/(cc-pVQZ plus augmented functions on *F* only) level, with all electrons correlated; see Ref. 4]. It was concluded that the best theoretical r_e agreed with the derived experimental value to ±0.0003 Å.

Second, in an *ab initio* study on F_2CC, Breidung and Thiel[9] reported CCSD(T)/aug-cc-pCVQZ (all electron) cal-

a)Electronic mail: bcftchau@polyu.edu.uk

culations on CF_2. This is at present the highest level of calculation on CF_2. The computed equilibrium geometry obtained at this level of calculation was $r_e = 1.2981$ Å and $\theta_e = 104.85°$ and was compared with the experimental equilibrium geometry derived by Margules *et al.*,[4] so as to establish error estimates in the computed r_e structure at the same level of calculation for F_2CC. It was concluded that computed geometrical parameters at this level of calculation are reliable to within 0.0006 Å and 0.04° for equilibrium bond lengths and angles, respectively.

Third, in an *ab initio* investigation of halocarbene, Schwartz and Marshall[10] carried out geometry optimization on a number of halocarbenes, including CF_2, at the QCISD/6-311G* level and quoted experimental equilibrium geometrical parameters of 1.3035±.0001 Å and 104.78 ±0.02° for the $\tilde{X}\,^1A_1$ state of CF_2.[11] It should be noted that these experimental values of r_e and θ_e are actually identical to the r_{av} and θ_{av} values of Kirchhoff *et al.*[8] determined by microwave spectroscopy; they are probably the averaged values rather than the equilibrium values.

Fourth, Sendt and Bacskay performed CASSCF, CASPT2, and CCSD(T) calculations on the $\tilde{X}\,^1A_1$, $\tilde{a}\,^3B_1$, and $\tilde{A}\,^1B_1$ states of CX_2, where X=F, Cl, and Br, employing the cc-pVTZ basis set.[12] Among a large number of computed spectroscopic constants, the discrepancies, which were significant, between the computed harmonic vibrational frequencies obtained at higher levels of calculation [CASPT2, CCSD(T), and also MRCI] and the observed fundamental frequencies of the two stretching modes of the $\tilde{A}\,^1B_1$ state of CF_2, particularly the asymmetric stretch, were discussed. The authors of this work were convinced that further improvement in the methodology and/or basis set would not reduce the discrepancies and suggested that they were probably due to the neglect of anharmonicities in the computed values. It should be mentioned that, in Ref. 1, we have discussed the large range of the computed values of the asymmetric stretching harmonic frequencies of the $\tilde{A}\,^1B_1$ state of CF_2 based on the results of our CASSCF and MP2 calculations and the earlier CASSCF results of Cameron *et al.*[13] It was pointed out that better agreement for the asymmetric stretch of the $\tilde{A}\,^1B_1$ state of CF_2 between the computed CASSCF harmonic frequencies and the observed fundamental frequency were only obtained with CASSCF calculations, which employed a large active space.[1] It appears that the shape of the potential energy surface in the asymmetric stretching coordinate of the $\tilde{A}\,^1B_1$ state of CF_2 is very sensitive to the level of calculation. It was also pointed out that the computed bond angle of the $\tilde{A}\,^1B_1$ state of CF_2 is sensitive to the level of calculation.[1]

Last, to our knowledge, the only PEFs available for CF_2 are the three-dimensional CASSCF/[$7s4p2d$] potential energy surfaces of the ground electronic state by Peterson *et al.*[14]

II. THEORETICAL CONSIDERATIONS AND COMPUTATIONAL DETAILS

The theoretical method employed in the anharmonic FCF code, AN-FCF, used in this study has been presented previously in Ref. 3. Therefore only an outline of the method and some technical details, which are specific to the present study, are given below.

For each electronic state involved in the emission process, the potential energy function, V, was determined by fitting the following polynomial to an appropriate number of CASSCF/MRCI/aug-cc-pVQZ(no g) or RCCSD(T)/aug-cc-pVQZ single point energies [for the $\tilde{A}\,^1B_1$ or $\tilde{X}\,^1A_1$ states of CF_2, respectively]:

$$V = \sum_{ij} C_{ij}(S_1)^i(S_2)^j + V_{eqm}. \tag{1}$$

The PEFs are expressed in terms of a Morse type coordinate:[15]

$$S_1 = [1 - e^{-\gamma(r - r_{eqm})/r_{eqm}}]/\gamma,$$

and a bending coordinate suggested by Carter and Handy:[16]

$$S_2 = \Delta\theta + \alpha\Delta\theta^2 + \beta\Delta\theta^3,$$

where r is the CF bond length, and $\Delta\theta$ is the displacement in the F–C–F bond angle. By restricting the gradient of S_2 to zero when the molecule is linear (i.e., $\theta = \pi$), the following expression relating to α and β can be obtained:[16]

$$\beta = [1 + 3\alpha(\pi - \theta_{eqm})^2]/[-2(\pi - \theta_{eqm})].$$

The nonlinear least-squares fit procedure,[17] NL2SOL, was employed to obtain the C_{ij}'s, V_{eqm}, r_{eqm}, θ_{eqm}, α, and γ from the computed single point energy data set. The asymmetric stretching modes of the two states considered have been ignored, because the observed SVL emission spectra do not show vibrational structure in the asymmetric stretch[2] and the computed FCFs involving the asymmetric stretching modes, obtained based on the harmonic oscillator model, have negligible relative intensities.[1]

Terms of up to the fifth order and also the C_{06} and the C_{60} terms were included in the PEF [Eq. (1)] of each of the two states involved in the emissions. As the SVL spectra consist of very long progressions in the bending mode of the ground electronic state, higher order terms in the bending mode, C_{07} and C_{08}, were added only to the PEF of the ground state. The numbers of single point RCCSD(T)/aug-cc-pVQZ total energies evaluated were 100 for the ground state of CF_2 covering ranges of $1.1\,\text{Å} \leqslant r \leqslant 1.745\,\text{Å}$ and $75° \leqslant \theta \leqslant 154°$. For the $\tilde{A}\,^1B_1$ state, 40 CASSCF/MRCI/aug-cc-pVQZ total energies covering the ranges of $1.1\,\text{Å} \leqslant r \leqslant 1.4\,\text{Å}$ and $91° \leqslant \theta \leqslant 160°$ were evaluated. The CASSCF/MRCI/aug-cc-pVQZ(no g) and RCCSD(T)/aug-cc-pVQZ energy calculations were performed using the MOLPRO suite of programs,[18,19] with three $1s$ core orbitals frozen in the correlation treatment. In the CASSCF and MRCI calculations[20,21] on the open-shell singlet excited $\tilde{A}\,^1B_1$ state, all valence orbitals were active. The MRCI energies including Davidson correction[22] were employed in obtaining the PEF. The CASSCF calculations considered 12 892 variables. The MRCI calculations had ~630 million uncontracted configurations and 3 million internally contracted configurations.

Variational calculations, which employed the rovibronic Hamiltonian for a nonlinear molecule of Watson,[23] were carried out to obtain the anharmonic vibrational wave functions. The latter were expressed as linear combinations of harmonic

oscillator functions, $h(v_1,v_2)$, where v_1 and v_2 denote the quantum numbers of the harmonic basis functions for the symmetric stretching and bending mode, respectively (see Ref. 3 for details). Harmonic basis functions up to $h(10,30)$ with the restriction of $v_1+v_2<30$ were employed for the ground state calculation. For the $\tilde{A}\,^1B_1$ state, harmonic basis functions of up to $h(10,15)$ with the restriction $v_1+v_2<15$ were used. The total numbers of basis functions used in the variational calculations were 286 and 121 for the $\tilde{X}\,^1A_1$ and $\tilde{A}\,^1B_1$ states of CF_2, respectively.

Since the anharmonic vibrational wave functions are expressed as linear combinations of harmonic basis functions, the anharmonic FCFs can be expressed in terms of the overlap integrals of the corresponding harmonic functions. The latter were evaluated by the method of Chen[24] (for details, see Refs. 1 and 3). Vibronic bands in the CF_2 SVL emission spectra, $\tilde{A}\,^1B_1 \rightarrow \tilde{X}\,^1A_1$, were simulated, using Gaussian functions with a full width at half maximum (FWHM) of 0.3 nm (28 cm^{-1} at 325 nm), and relative intensities as given by the corresponding computed anharmonic FCFs.

The iterative Franck–Condon analysis (IFCA) procedure was carried out in the spectral simulation of each SVL emission employing the AN-FCF code (see Ref. 3 for details). In the IFCA procedure, the geometry of the $\tilde{X}\,^1A_1$ state was fixed to the available experimental equilibrium geometry. The geometrical parameters of the $\tilde{A}\,^1B_1$ state were initially chosen according to the computed geometry change on excitation from *ab initio* calculations and were then varied, over a small range, systematically, until a best match between the simulated and observed spectra was achieved. In Ref. 1, experimentally derived geometrical parameters of the $\tilde{A}\,^1B_1$ state of CF_2 were obtained from the IFCA procedure, employing the harmonic CART-FCF code. However, a good match between the simulated and observed spectra was only achieved for a few vibrational components with low quantum numbers in the ground electronic state. In the present study with the AN-FCF code, it was possible to obtain a good match throughout the whole spectral band (see Sec. III). In Ref. 1, the r_0 geometry of Mathews[25] was employed for the $\tilde{X}\,^1A_1$ state in the IFCA procedure. In the present study, with the recently available experimentally derived equilibrium geometrical parameters of Margules *et al.*,[4] the geometry of the $\tilde{X}\,^1A_1$ state of CF_2 was fixed at $r_e = 1.2975$ Å and $\theta_e = 104.8°$ in the IFCA procedure. Based on the two sets of experimentally derived geometrical parameters given in Ref. 4 (see Sec. I), upper limits of the uncertainties associated with these ground state geometrical parameters are probably around ± 0.0010 Å and $\pm 0.1°$ for r_e and θ_e respectively.

TABLE I. CASSCF/MRCI/aug-cc-pVQZ(no *g*) and RCCSD(T)/aug-cc-pVQZ PEF of the $\tilde{A}\,^1B_1$ and $\tilde{X}\,^1A_1$ states of CF_2, respectively.[a]

Parameters	$\tilde{X}\,^1A_1$	$\tilde{A}\,^1B_1$
C_{20}	3.0469	2.7504
C_{11}	0.3986	0.1350
C_{03}	0.2710	0.1241
C_{30}	−5.6472	10.6753
C_{21}	−1.7372	−0.0997
C_{12}	−1.0191	−0.4177
C_{03}	−0.0698	−0.0213
C_{40}	6.2001	48.4845
C_{22}	1.5673	−0.7977
C_{04}	0.2528	0.0373
C_{31}	0.5872	0.2078
C_{13}	2.1408	0.6084
C_{05}	0.1008	0.0984
C_{06}	−0.4663	0.3177
C_{50}	−1.7222	148.2864
C_{60}	−3.2016	181.0831
C_{41}	−0.3516	3.6957
C_{32}	−1.5753	−0.9673
C_{23}	−1.8493	−0.4355
C_{14}	−0.8155	−0.4291
C_{07}	−0.0887	⋯
C_{08}	1.3159	⋯
r_{eqm}/Å	1.3008	1.3215
θ_{eqm}/°	104.754	121.980
α/radian^{-1}	−0.0516	−0.1944
γ	1.3151	6.9581

[a]For each state, the rms deviation of the fitted PEF from the *ab initio* total energies is <10 cm^{-1}. The units for C_{ij} are hartree radian^{-1}.

TABLE II. Anharmonic vibrational wave functions and energies (cm^{-1}) of the first four vibrational levels and the $|0,17\rangle$ level of the $\tilde{X}\,^1A_1$ state of CF_2.

Level[a]	Energy	Wave function
$\|0,17\rangle$	11 229.632	0.3372h(0,17)−0.2994h(1,15)−0.2570h(0,22) −0.2463h(0,21)+0.2344h(0,18)+0.2300h(0,14) −0.2195h(0,23)−0.2112h(0,20)−0.1972h(0,13) +0.1937h(1,17)+0.1932h(1,18)−0.1825h(0,16) −0.1750h(0,15)−0.1673h(0,24)+0.1617h(2,13) +0.1543h(0,12)−0.1489h(2,15)−0.1477h(1,12) +0.1467h(1,19)+0.1428h(1,13)−0.1223h(0,25) +0.1156h(1,11)+0.1026h(1,20)
$\|0,2\rangle$	1336.254	−0.9696h(0,2)−0.1937h(0,3)+0.1172h(0,1)
$\|1,0\rangle$	1231.106	0.9870h(1,0)+0.1031h(2,0)+0.0931h(1,1)
$\|0,1\rangle$	668.275	−0.9902h(0,1)−0.1179h(0,2)+0.0536h(0,0)
$\|0,0\rangle$	0.0	0.9977h(0,0)+0.0536h(0,1)+0.0379h(1,0)

[a]Notation used here is $|v_1,v_2\rangle$ for the anharmonic wave function, where v_1 is the vibrational quantum number in the symmetric stretching mode and v_2 is the vibrational quantum number in the symmetric bending mode.

TABLE III. Comparison of the observed and computed vibrational energies of the $\tilde{X}\,^1A_1$ state of CF_2 obtained from SVL emission spectra (Ref. 2), CASSCF PEF (Ref. 14) and CCSD(T) PEF (this work).

$\lvert v_1,v_2,v_3\rangle$	Observed (average)[a]	Std. dev.[a]	CASSCF	RCCSD(T)
0,1,0	659	20	674	668
1,0,0	1189	47	1230	1231
0,2,0	1327	30	1347	1336
1,1,0	1837	35	1898	1894
0,3,0	1976	20	2019	2003
1,2,0	2477	53	2565	2556
0,4,0	2640	43	2690	2671
1,3,0	3188	32	3232	3218

[a]The numbers shown are the averaged values of the observed vibrational spacings in the $\tilde{X}\,^1A_1$ state of CF_2, obtained from emissions originated from different vibrational levels of the $\tilde{A}\,^1B_1$ state, as given in Ref. 2. Note that the measured vibrational spacings obtained from different SVL emissions, as given in Ref. 2, are not the same for the same pairs of vibrational levels in the $\tilde{X}\,^1A_1$ state. Presumably the discrepancies are due to experimental uncertainties, whose magnitudes are reflected in the standard deviations obtained when taking the averages.

III. RESULTS AND DISCUSSION

The PEFs of the $\tilde{A}\,^1B_1$ and $\tilde{X}\,^1A_1$ states of CF_2 are given in Table I. With the selected C_{ij} terms, and r and θ ranges given above, the rms deviations of the fitted PEF from the computed *ab initio* energies are within 10 cm^{-1} for both electronic states. The anharmonic vibrational wave functions of the first four vibrational levels $\lvert v_1,v_2\rangle$, and the anharmonic level, $\lvert 0,17\rangle$, of the $\tilde{X}\,^1A_1$ state, and their computed energies are given in Table II. (The highest observable level of the $\tilde{X}\,^1A_1$ state in the SVL emission spectra has v_2 at around 17.) With harmonic basis functions of up to $h(10,30)$, as given above, the computed vibrational energy of the $\lvert 0,17\rangle$ anharmonic level converged to within 1 cm^{-1} in the variational calculation. The effects of a larger harmonic basis set [up to $h(10,50)$] on the computed vibrational energies and anharmonic wave functions were also checked and were found to be negligible.

The deviation of the coefficient of the leading harmonic basis function from unity is a measure of the magnitude of anharmonic effects in the corresponding anharmonic vibrational wave function. In Table II, it can been seen that anharmonic effects are significant, even for low-lying anharmonic vibrational levels of the $\tilde{X}\,^1A_1$ state of CF_2. For the anharmonic $\lvert 0,17\rangle$ level, all harmonic functions with coefficients larger than 0.1 are included in Table II. The highest quantum number of the harmonic basis function, which has a significant contribution (with a coefficient of larger than 0.1), to this anharmonic level, is $v_2=25$. The $h(0,26)$ harmonic function has a coefficient of -0.0846, while all $h(0,v_2)$

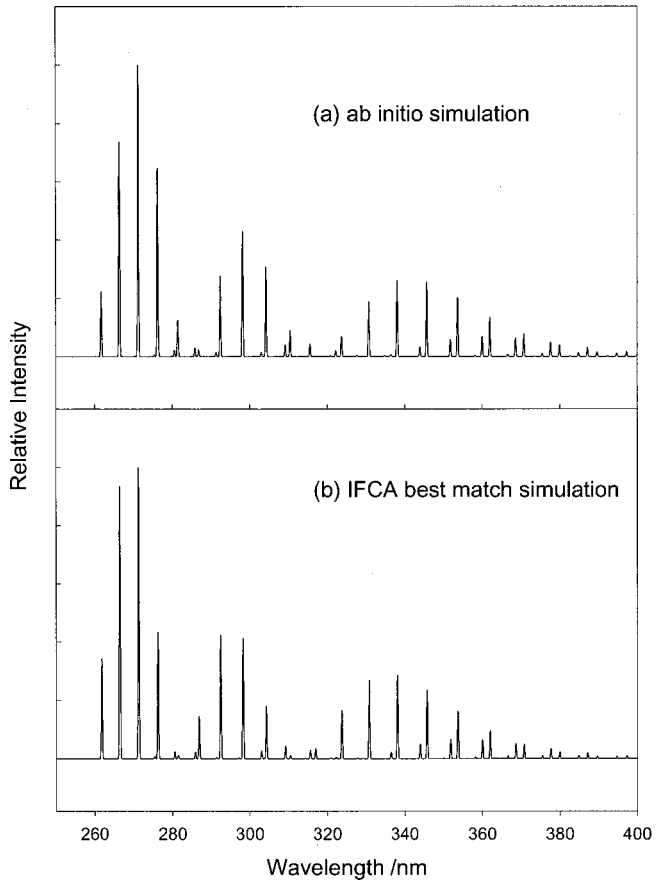

FIG. 1. Simulated spectra of the $\tilde{A}\,^1B_1(0,2,0)\rightarrow\tilde{X}\,^1A_1$ CF_2 single vibronic level (SVL) emission: (a) employing the CASSCF/MRCI/aug-cc-pVQZ(no *g*) and RCCSD(T)/aug-cc-pVQZ geometries for the two states, respectively, and (b) employing the experimental equilibrium geometry from Ref. 4 for the $\tilde{X}\,^1A_1$ state and the IFCA geometry of r_e(CF)=1.317 Å and θ_e(FCF) =121.25° for the $\tilde{A}\,^1B_1$ state.

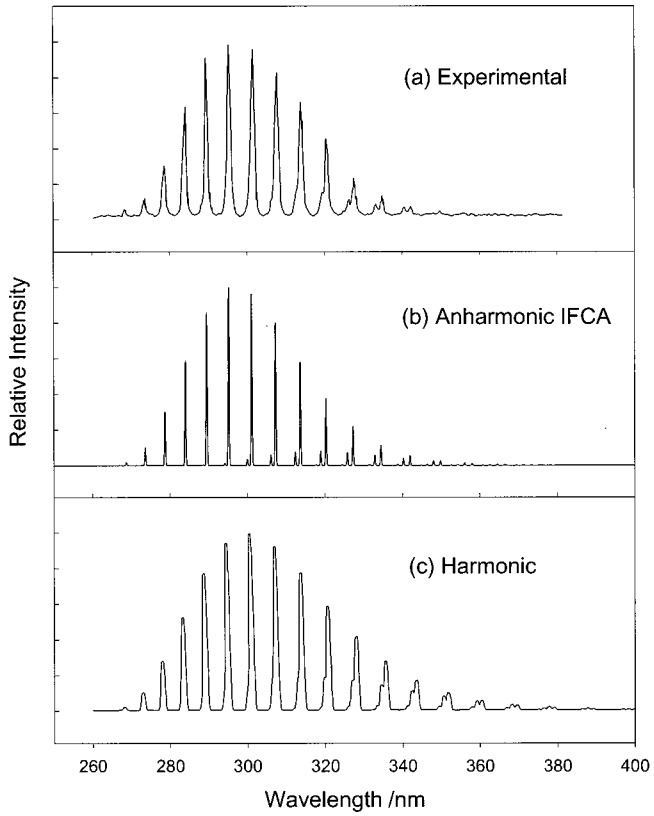

FIG. 2. $\tilde{A}\,^1B_1(0,0,0)\rightarrow\tilde{X}\,^1A_1$ CF_2 single vibronic level (SVL) emission: (a) experimental spectrum from Ref. 2, (b) simulated spectrum including anharmonicity and employing the IFCA geometry of r_e(CF)=1.317 Å and θ_e(FCF)=121.25° for $\tilde{A}\,^1B_1$ state, and (c) simulated spectrum based on the harmonic oscillator model [with MP2 force constants and the IFCA geometry of r_e(CF)=1.318 Å and θ_e(FCF)=121.6°; Fig. 1 of Ref. 1].

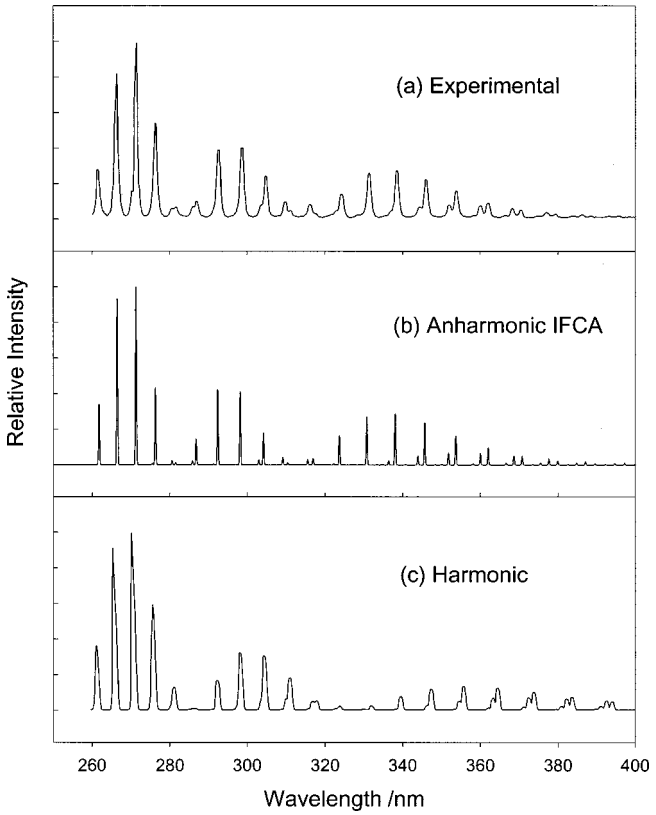

FIG. 3. $\tilde{A}\,^1B_1(0,2,0)\rightarrow\tilde{X}\,^1A_1$ CF_2 single vibronic level (SVL) emission: (a) experimental spectrum from Ref. 2, (b) simulated spectrum including anharmonicity and employing the IFCA geometry of $r_e(\mathrm{CF})=1.317$ Å and $\theta_e(\mathrm{FCF})=121.25°$ for $\tilde{A}\,^1B_1$ state, and (c) simulated spectrum based on the harmonic oscillator model [with MP2 force constants and the IFCA geometry of $r_e(\mathrm{CF})=1.318$ Å and $\theta_e(\mathrm{FCF})=121.6°$; Fig. 1 of Ref. 1].

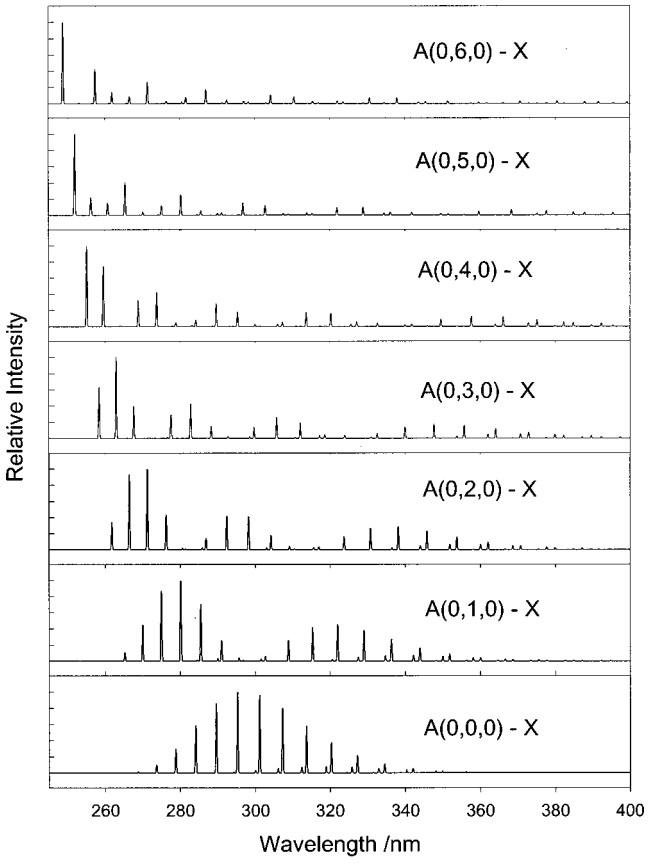

FIG. 4. Simulated spectra of the $\tilde{A}\,^1B_1(0,v_2,0)\rightarrow\tilde{X}\,^1A_1$ CF_2 single vibronic level (SVL) emissions, for $v_2=0-6$, employing the CASSCF/MRCI/aug-cc-pVQZ(no *g*) and RCCSD(T)/aug-cc-pVQZ PEF for the two states, respectively, the experimental geometry from Ref. 4 for the $\tilde{X}\,^1A_1$ state and the IFCA geometry of $r_e(\mathrm{CF})=1.317$ Å and $\theta_e(\mathrm{FCF})=121.25°$ for the $\tilde{A}\,^1B_1$ state.

functions with v_2 larger than 26 have coefficients smaller than 0.05. From the computed anharmonic vibrational wave function of the $|0,17\rangle$ level, it can be concluded that the harmonic basis functions employed in the variational calculations are adequate for the purpose.

Calculated low-lying anharmonic vibrational energies for the first eight levels for excitation in the symmetric stretching mode (ν_1) and the symmetric bending mode (ν_2) relative to the $|0,0,0\rangle$ level of the $\tilde{X}\,^1A_1$ state of CF_2, employing the RCCSD(T) PEF reported, are shown in Table III together with those of the CASSCF PEF from Ref. 14. The vibrational energies determined from the SVL spectra of King *et al.*[2] are also included in Table III for comparison. The experimental vibrational energies of the $\tilde{X}\,^1A_1$ state of CF_2, given in Table III, are averages obtained from different SVL spectra from different vibrational levels of the $\tilde{A}\,^1B_1$ state (see footnote to Table III). Based on comparison of calculated and averaged experimental vibrational energies, our CCSD(T) PEF appears to be slightly superior to the CASSCF PEF of Peterson *et al.*[14] We have also employed the CASSCF PEF of the $\tilde{X}\,^1A_1$ state of CF_2 [instead of our RCCSD(T) PEF; see the later text] in the anharmonic FCF calculations. The simulated spectra thus obtained are very similar to those obtained employing our RCCSD(T) PEF; small deviations in the relative component intensities between the two simulations arise only from transitions to v_2'' $\geqslant 8$. Comparison between the simulated and observed spectra suggests that the simulated spectra employing the RCCSD(T) PEF are slightly superior to those with the CASSCF PEF in the high wavelength region. Subsequently, we will concentrate on the spectral simulations employing our RCCSD(T) PEF for the $\tilde{X}\,^1A_1$ state.

Some selected simulated spectra are shown in Figs. 1–4. Figure 1(a) shows the ''purely'' theoretical spectrum of the $\tilde{A}(0,2,0)\rightarrow\tilde{X}$ emission, employing the CASSCF/MRCI and RCCSD(T) equilibrium geometries for the $\tilde{A}\,^1B_1$ and $\tilde{X}\,^1A_1$ states of CF_2, respectively, (see Table I). Figure 1(b) shows the simulated spectrum, which best matches the experimental $\tilde{A}(0,2,0)\rightarrow\tilde{X}$ emission spectrum, obtained with the experimental equilibrium geometry for the $\tilde{X}\,^1A_1$ state and the IFCA geometry of $r_e=1.317$ Å and $\theta_e=121.25°$ for the $\tilde{A}\,^1B_1$ state. The differences between these two simulations are significant. On one hand, these spectra demonstrate the sensitivity of computed FCFs to the relative geometries of the electronic states involved in the transition. On the other hand, they suggest that there is still a small difference between the *ab initio* relative geometrical parameters of the two states and the true ones.

In Figs. 2 and 3, the observed $\tilde{A}(0,2,0)\rightarrow\tilde{X}$ and

TABLE IV. Summary of some computed and experimental geometrical parameters and vibrational frequencies (cm^{-1}) of the $\tilde{A}\,^1B_1$ and $\tilde{X}\,^1A_1$ states of CF_2.

$\tilde{X}\,^1A_1$	r_e/Å	θ_e/°	ω_1	ω_2	ω_3
CCSD(T)/aug-cc-pVQZ	1.301	104.8	1242	670	⋯
(as above) fundamental			1231	668	
MP2/6-311+G(2df)[a]	1.298	105.0	1261	679	1151
CASPT2/cc-pVTZ[b]	1.300	105.2	1245.4	671.0	1163.0
CCSD(T)/cc-pVTZ[b]	1.303	104.9	1255.2	672.9	1162.5
CCSD(T)/cc-pVQZ+ aug(F); (all electrons)[c]	1.2972	104.85			
CCSD(T)/aug-cc-pCVQZ; (all electrons)[d]	1.2981	104.85			
Expt.	1.2975[c]	104.81[c]	1225.0793[e]	666.24922[e]	1114.4435[e]
Expt. (r_0)[f]	1.300	104.94			
Expt. (r_{av})[g]	1.3035	104.778			
$\tilde{A}\,^1B_1$					
CASSCF/MRCI/ aug-cc-pVQZ(no g)	1.322	122.0	1058	500	⋯
(as above) fundamental			1042	496	
MP2/6−311+G(2df)[a]	1.308	120.9	1173	523	1405
CASPT2/cc-pVTZ[b]	1.319	122.4	1062.3	499.1	1290.1
Expt (r_0)	1.316[h]	122.3[h]	1011[e]	496[e]	1180[e]
IFCA-MP2[a,i]	1.318	121.6			
IFCA-CASSCF[a,i]	1.316	122.4			
IFCA[j]	1.317	121.25			

[a]Reference 1.
[b]Reference 12.
[c]Reference 4; all electrons correlated.
[d]Reference 9; all electrons correlated.
[e]Reference 13.
[f]Reference 25.
[g]Reference 8.
[h]Reference 26.
[i]IFCA geometries of the $\tilde{A}\,^1B_1$ state were obtained employing the CART-FCF code, with the MP2 and CASSCF force constants, respectively, reference 1 for details.
[j]From the present study, employing the ANF-FCF code, with the CASSCF/MRCI and RCCSD(T) PEF for the $\tilde{A}\,^1B_1$ and $\tilde{X}\,^1A_1$ states of CF_2 respectively.

$\tilde{A}(0,0,0)\rightarrow\tilde{X}$ emissions [Figs. 2(a) and 3(a), respectively], are compared with the corresponding simulated spectra obtained previously within the harmonic oscillator model[1] [Figs. 2(c) and 3(c)] and those obtained in the present study with anharmonicity included in the FCF calculations [Figs. 2(b) and 3(b)]. (Each of the simulated spectra employed the respective IFCA geometry for the $\tilde{A}\,^1B_1$ state; see figure captions of Figs. 2 and 3.) It is pleasing to see that the agreement between the simulated and observed spectra is much improved when anharmonicity is included. As mentioned above, an excellent match between the simulated and observed spectra can be obtained throughout the whole spectral band for each SVL emission. The whole series of SVL $\tilde{A}(0,v_2',0)\rightarrow\tilde{X}$ emissions, where $v_2'=0$ to 6, reported by King *et al.*,[2] have been simulated and are shown in Fig. 4. The agreement between the simulated and observed spectra for the whole series of SVL emissions is very good.

IV. CONCLUDING REMARKS

Following our preliminary work on the spectral simulations of $\tilde{A}\rightarrow\tilde{X}$ CF_2 SVL emissions, we have replaced the harmonic oscillator model used with an anharmonic model and obtained simulated spectra which include anharmonicity. The significant improvement in the simulated spectra presented in this work confirms that the discrepancies between previously reported simulated spectra obtained within the harmonic oscillator model and the observed spectra are mainly due to the lack of allowance for anharmonicity in the electronic states in the previous FCF calculations. In this study, the CASSCF/MRCI/aug-cc-pVQZ(no g) and RCCSD(T)/aug-cc-pVQZ PEFs employed in the FCF calculations are also of a higher level than the MP2/6-311+G(2df) and CASSCF/6-31G* calculations used in Ref. 1.

The excellent agreement throughout the whole spectral range between the simulated spectra obtained here and the observed $\tilde{A}\rightarrow\tilde{X}$ CF_2 SVL emission spectra reported in Ref. 2 is very encouraging. This also suggests that the changes of electronic transition moment across the spectral bands are probably negligibly small. In this connection, the reliability of the IFCA geometry of the $\tilde{A}\,^1B_1$ state obtained from the present study employing the AN-FCF code is significantly strengthened, as the match between the simulated and observed spectra is now almost perfect. Merely based on comparison of the slightest observable changes in the simulated relative intensities with the smallest changes in the IFCA geometrical parameters, upper limits of the uncertainties associated with the IFCA geometrical parameters are estimated

to be ± 0.003 Å and $\pm 0.3°$ in r_e and θ_e, respectively, in the $\tilde{A}\,^1B_1$ state of CF_2.

Optimized geometrical parameters and computed vibrational frequencies of the two electronic states of CF_2 considered, obtained at the highest levels of calculations, and the corresponding experimentally derived values are summarized in Table IV. The highest level of calculation on the $\tilde{X}\,^1A_1$ state of CF_2 is the RCCSD(T)/aug-cc-pCVQZ (all electrons correlated) level from Ref. 9. However, vibrational frequencies are not available at this level. The RCCSD(T)/aug-cc-pVQZ level of calculation from the present study is the highest level for computed vibrational frequencies of the $\tilde{X}\,^1A_1$ state. For the $\tilde{A}\,^1B_1$ state of CF_2, the CASSCF/MRCI/aug-cc-pVQZ(no *g*) level of this work is the highest level of calculation performed to date. Regarding equilibrium geometrical parameters of the $\tilde{A}\,^1B_1$ state, the IFCA values obtained from this work should be the most reliable. For both electronic states, the agreement between the computed geometrical parameters obtained at the CASSCF/MRCI/aug-cc-pVQZ(no *g*) or RCCSD(T)/aug-cc-pVQZ levels from this work and the available experimental values are in general fairly good, with bond lengths agreeing to within 0.004 Å and the bond angle agreeing to within 0.7°. Regarding vibrational frequencies, we have obtained not only harmonic values, but also fundamentals in the present study for the symmetric stretching and bending modes of both the $\tilde{X}\,^1A_1$ and $\tilde{A}\,^1B_1$ states of CF_2. The agreement between the computed and observed fundamental frequencies is within ~ 30 cm^{-1}. In general, the computed fundamental frequencies agree better with the experimental values than the computed harmonic ones, as expected. Regarding the CASSCF/MRCI and RCCSD(T) PEFs reported here, although the asymmetric stretching coordinate has not been considered and the ranges of the bond length covered in the energy scans for the two states may be considered as narrow, the excellent match between the simulated spectra employing these PEFs and the observed spectra suggest that these PEFs are adequate for the purpose of FCF calculations; they are at present the highest level PEFs available for the two states of CF_2.

The results of this work, and the results of our earlier article on the simulation of the UV photoelectron bands of ClO_2 with this method,[3] strongly suggest that this approach can be applied with confidence to electronic and photoelectron spectra of other small polyatomic molecules.

ACKNOWLEDGMENTS

The authors are grateful to the Research Grant Council (R.G.C.) of the Hong Kong Special Administrative Region (Project POLYU 5180/99P and 5187/00P) and the Research Committee of the Hong Kong Polytechnic University. Support from the EPSRC(UK) and the Leverhulme Trust are also acknowledged.

[1] F. T. Chau, J. M. Dyke, E. P. F. Lee, and D. C. Wang, J. Electron Spectrosc. Relat. Phenom. **97**, 33 (1998).
[2] S. D. King, P. K. Schenck, and J. C. Stephenson, J. Mol. Spectrosc. **78**, 1 (1979).
[3] D. K. W. Mok, E. P. F. Lee, F. T. Chau, D. C. Wang, and J. M. Dyke, J. Chem. Phys. **113**, 5791 (2000).
[4] L. Margules, J. Demaison, and J. E. Boggs, J. Phys. Chem. A **103**, 7732 (1999).
[5] A. Charo and F. C. DeLucia, J. Mol. Spectrosc. **94**, 363 (1982).
[6] J. B. Burholder, C. J. Howard, and D. A. Hamilton, J. Mol. Spectrosc. **127**, 362 (1988).
[7] H.-B. Qian and D. B. Davies, J. Mol. Spectrosc. **169**, 201 (1995).
[8] W. H. Kirchhoff, D. R. Lide, Jr., and F. X. Powell, J. Mol. Spectrosc. **47**, 491 (1993).
[9] J. Breidung and W. Thiel, J. Mol. Spectrosc. **205**, 28 (2001).
[10] M. Schwartz and P. Marshall, J. Phys. Chem. A **103**, 7900 (1999).
[11] *Thermodynamic Properties of Individual Substances*, edited by L. Gurvich, I. V. Veyts, and C. B. Alcock (Hemisphere, New York, 1992), Vol. 2.
[12] K. Sendt and G. B. Bacskay, J. Chem. Phys. **112**, 2227 (2000).
[13] M. R. Cameron, S. H. Kable, and G. B. Bacskay, J. Chem. Phys. **103**, 4476 (1995).
[14] K. A. Peterson, R. C. Mayrhofer, E. L. Sibert III, and R. C. Woods, J. Chem. Phys. **94**, 414 (1991).
[15] W. Meyer, P. Botschwina, and P. Burton, J. Chem. Phys. **84**, 891 (1986).
[16] S. Carter and N. C. Handy, J. Chem. Phys. **87**, 4294 (1987).
[17] J. E. Dennis, Jr., D. M. Gay, and R. E. Welsh, ACM Trans. Math. Software **7**, 348 (1981); *ibid.* **7**, 369 (1981).
[18] MOLPRO is a package of *ab initio* programs by H.-J. Werner and P. J. Knowles, with contributions from J. Almlöf, R. D. Amos, A. Berning *et al.*
[19] P. J. Knowles, C. Hampel, and H. J. Werner, J. Chem. Phys. **99**, 5219 (1993).
[20] H.-J. Werner and P. J. Knowles, J. Chem. Phys. **82**, 5053 (1985).
[21] H.-J. Werner and P. J. Knowles, J. Chem. Phys. **89**, 5803 (1988).
[22] E. R. Davidson, Chem. Phys. Lett. **52**, 403 (1977).
[23] J. K. G. Watson, Mol. Phys. **19**, 465 (1970).
[24] P. Chen, in *Unimolecular and Bimolecular Reaction Dynamics*, edited by C. Y. Ng *et al.* (Wiley, New York, 1994), pp. 371–425.
[25] C. W. Matthews, Can. J. Phys. **45**, 2355 (1967).
[26] F. J. Comes and D. A. Ramsay, J. Mol. Spectrosc. **113**, 495 (1985).